JTE HCMUTE
ISSN: 2615-9740

JOURNAL OF TECHNICAL EDUCATION SCIENCE
Ho Chi Minh City University of Technology and Education
Website: https://jte.hcmute.edu.vn/
Email: jte@hcmute.edu.vn

Multi-Range Fusion for X-ray Image Enhancement

Ngoc-Tham Vo[1], Kim-Hoanh Ly[2], Manh-Hung Nguyen[1*]

[1] *HCMC University of Technology and Education, Vietnam*

[2]*Da Nang University, Da Nang, Vietnam*

[*] Corresponding author. *Email: hungnm@hcmute.edu.vn*

ARTICLE INFO

Received: 19/12/2021
Revised: 9/2/2022
Accepted: 9/2/2022
Published: 28/2/2022

KEYWORDS

X-ray image;
Fusion;
Contrast;
Preserving information;
Enhancement.

ABSTRACT

Digital medical images are stored in the Digital Imaging Communications in Medicine (DICOM) standard where a 12-bit integer represents each pixel. However, commercial display devices are only designed to work with an 8-bit standard such as JPEG or PNG. Traditional methods compress the high dynamic range (HDR) to a low dynamic range (LDR) to visualize a DICOM image. The compression process is a linear transformation and the LDR is represented in an 8-bits format. Due to a quantization error the contrast is limited. Therefore, in this article, we propose a method to enhance X-ray images in term of contrast. Firstly, we estimate an information range that captures valuable information of an x-ray image. The range is represented by an upper and lower threshold. Within these thresholds, LDR images will be extracted to capture information from a specific sub-range. These images are then fused to create an enhanced LDR image that has a higher contrast but retains information from each sub-range. Experimental results demonstrate that the proposed method helps achieve a better contrast.

Doi: https://doi.org/10.54644/jte.68.2022.1099

1. Introduction

Using x-ray images is an economical but effective method to help doctors diagnose the patient's status early. Typically, x-ray machines capture and store images in DICOM standard that represents each pixel by a 12-bit integer. Conventional methods compress a DICOM image to common 8-bit formats to display the image on commercial screens. In detail, the maximum and minimum values in the DICOM image are mapped to 255 and 0 correspondingly.

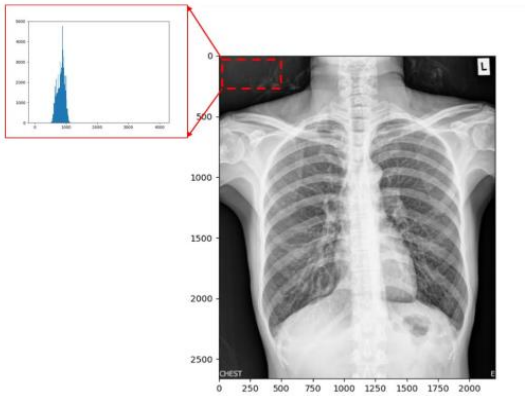

Figure 1. *The dark area (red rectangle) contains no useful information but have a high value of gray level*

JTE
HCMUTE
ISSN: 2615-9740

JOURNAL OF TECHNICAL EDUCATION SCIENCE
Ho Chi Minh City University of Technology and Education
Website: https://jte.hcmute.edu.vn/
Email: jte@hcmute.edu.vn

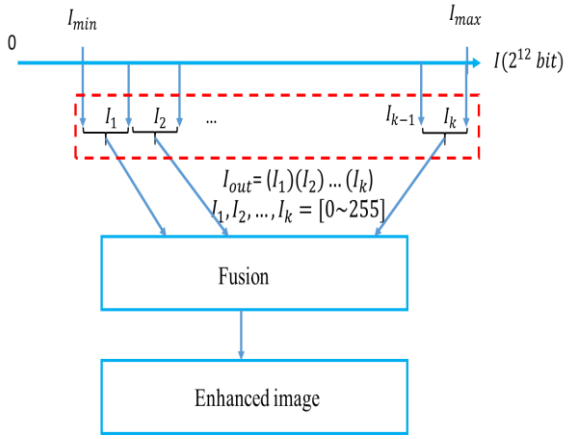

Figure 2. *Flowchart of proposed image enhancement method*

Conventional enhancement methods [1] enhance the image contrast while minimizing negative effects such as halo or color distortion. However, the contrast enhancement is limited due to its global transform. Local transforms [2]-[3] tend to improve the contrast level but cause the halo effect and change the image structure. In addition, in a medical application, the image contrast may not be the only quality that a doctor would like to consider. An x-ray image, physically, measures the amount of energy left over by an x-ray beam as it passes through an object. The heavier object, the more energy is absorbed. Therefore, the x-ray image reflects the mass of objects that the x-ray beam passes. For example, in Figure 1, the bright region represents areas where many muscles and bones are crowded, and the dark area represents air. Maintaining this information area will, in some ways, contribute to diagnosis and treatment. Huang [4], [5] have proposed an enhancement method that preserves the mass information. The method relied on a normalization that only considered the maximum value of the original DICOM image. Because the minimum value of a DICOM image may not consider any meaningful information, ignoring the minimum value leads to wasting ranges to visualize unnecessary information. For instance, the histogram in Figure.1 points out that gray values of less information area are not zeros. That means there exists a lower bound that only pixels greater than the value could involve useful information. Determining this threshold will help to save more space for visualization.

Behind the existence of an information range in a DICOM image, the quantization error during a linear transformation will reduce the contrast and sharpness of normalized images. Instead of using linear normalization as [4], [5], we propose to split the essential range into sub-ranges, as shown in Figure 2. Then, each sub-range will be represented by an 8-bit image. Finally, the 8-bit images are fused to generate a well-enhanced LDR image.

In summary, three main contributions in this paper can be summarized as follows:

(a) We propose an enhancement method by estimating an information range of the original x-ray image. By evaluating this range, we can filter out the no useful information region in the image and have more space to enhance the image.
(b) To avoid missing information by quantization error. A fusing process is introduced to combine multiple images from sub-ranges.
(c) Experimental results on various images prove that our method can get a better result in terms of contrast level to the original one.

2. Relative works

2.1 Conventional enhancement methods.

Several methods enhance the image contrast, such as global mapping [1], local mapping [2]. The global mapping uses a global function to convert the gray input values into the output while expanding the global contrast. Because this transform function is globally applied over the entire image, the details

may not be enhanced well. In contrast, local tone mapping methods enhance an image based on the neighboring information. This property ensures the contrast is increased in every local patch. However, the general image can produce undesired block effects.

2.2 HDR Tone Mapping

A DICOM image uses a 12-bit integer to represent a pixel. Hence, we may treat it as an HDR image. Furthermore, the HDR tone mapping method [6], [7] could compress the image to an LDR image. Given multiple LDR images captured by commercial cameras, the HDR technique tries to create a synthesis LDR image that is high quality. There are two solutions for compression processing. In the first approach, an HDR image is reconstructed through a camera respond function (CDF); then, a tone-mapping method [6], [7] is used to compress the high dynamic range image to a lower one. On the other hand, the second approach [8] directly produces the synthesis LDR image based on the captured LDR images instead of reconstructing an HDR image. Here, a quality map is estimated for each captured LDR image. Based on the quality maps, the synthesis LDR is fused linearly.

In our method, we apply the second approach to render a synthesis LDR image. However, unlike the conventional fusion method that component LDR images are already available, our method does not have LDR images as inputs. Therefore, we select sub-ranges in an important information range and use the range to render component LDR images.

2.3 Enhancement for X-ray image

Recently, several methods have been specially developed to enhance an x-ray image. In [3], Koonsanit introduces a local enhancement method that focuses on the contrast of a local region. Huang [4] removes redundant tissues to enhance valuable components. However, the brightness of the image also is reduced. An extended version of [4] has been introduced in [5] to preserve the mass information and ensure the brightness of the image is preserved. Here, the model had been modified to ensure the maximum local value of the image will be similar after enhancement. By introducing this constraint, the method in [5] could improve the contrast while preserving mass information.

2.4 Deep learning-based enhancement

Recently, deep learning-based methods have achieved remarkable success in image restoration and enhancement. Compared to the conventional enhancement framework, the deep-learning-based methods have their advantage and drawback.

The conventional image enhancement method can provide a vivid result, but the result has highly relied on control parameters. Because it is difficult to select suitable control parameters for all images, an expert may need to select these parameters manually. In contrast, deep-learning-based methods can work without parameter selection. Because a network can approximate the control parameters, a non-expert user can quickly get a brilliant image without a deep understanding of the enhancement algorithm.

However, to train a deep-learning-based model, a label is needed. In the scenario of enhancement or compression task, pair-wise images must be provided [9]. The pair-wise images include an input image and its corresponding enhanced image. Here the enhanced image is provided by an expert. Recently, the state-of-the-art method [10] may not require pair-wise images but need a set of enhanced images to train a Generative Adversarial Networks [11] model. However, the performance would not be comparable with methods that use pair-wise images to train the network.

3. Proposed method

3.1 Overview of the proposed model

The overview of the proposed method is briefly described in Figure 3. Firstly, the important range is estimated automatically. This range defines which interval that most information is stored. Later, sub-ranges from the important range are extracted, and component LDR images are rendered from these ranges. This rendering image serves as images captured by different exposure times in conventional

JTE
HCMUTE
ISSN: 2615-9740

JOURNAL OF TECHNICAL EDUCATION SCIENCE
Ho Chi Minh City University of Technology and Education
Website: https://jte.hcmute.edu.vn/
Email: jte@hcmute.edu.vn

HDR compression. Next, quality maps that represent pixel qualities of component images are estimated by the saturation score [8] and contrast score [8]. Finally, the fusion mechanism [8] is used to combine these images into a better result.

3.2 Important range estimation

The range is defined by a lower bound and bound and an upper bound. Due to the peculiarity of X-ray images that bright areas contain more important information, in [5], the upper bound is chosen as the maximum value in the image. Hence, the upper bound I_{im}^{max} of the range is $I_{im}^{max} = \max(I)$.

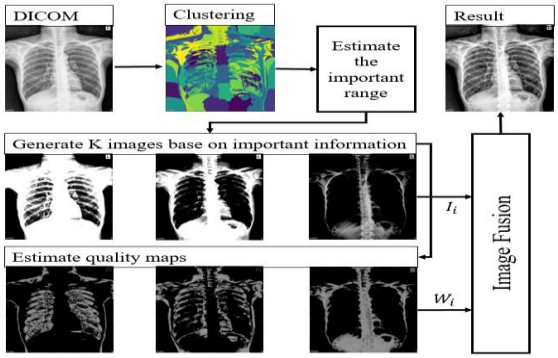

Figure 3. *Image enhance system based on the proposed method*

Unlike the previous work [5], where the lower bound is zero, one of our contributions is automatically selecting a suitable lower bound. To determine the lower bound, we base on the missing curve as in Figure 4. Here, the x-axis represents the relative lower bound, and the y-axis represents the missing information. Using this curve, we ensure the losing information ratio will not be greater than a δ threshold given the selected lower bound.

To estimate the curve, we first segment the original DICOM image into several groups that are represented by gray levels. Later, the amount of missing information is measured by entropy metric [12]. In detail, we model each pixel by three features F. These features are normalized to the interval [0,1] as equations (1), (2), (3), and (4).

$$F_0 = I_{i,j}/\max(I) \quad (1)$$

$$F_1 = i/D \quad (2)$$

$$F_2 = j/D \quad (3)$$

$$D = \sqrt{M^2 + N^2} \quad (4)$$

Here, $I_{i,j}$ is the gray value of the pixel at the i^{th} row and the j^{th} column; M and N are the numbers of rows and columns of the image. We use the Gaussian Mix Model clustering [13] to group pixels into different clusters. Denote F^k is the center of the k^{th} cluster of the original DICOM image, the F_0^k is the gray level represents the mask of this cluster. Each value $F_0^k\{k = 1 \sim K\}$ is a possible lower bound that we aim to estimate.

Given two neighbor cluster centers $[F_0^k, F_0^{k+1}]$, we extract a component image from the interval $[F_0^k, F_0^{k+1}]$ as Equation (5); and the information $E_{c_k,c_{k+1}}$ of this interval estimated by entropy as in Equation (6). The term $E_{c_k,c_{k+1}}$ represents the information in the image $I_{c_k,c_{k+1}}$. A better image, a greater entropy will have.

$$I_{c_k,c_{k+1}} = 255 * Clip\left(\frac{I-c_k}{c_{k+1}-c_k}; low = 0, high = 1\right) \quad (5)$$

$$E_{c_k,c_{k+1}} = -\sum_{r=0}^{255} p_r(I_{c_k,c_{k+1}}) \log_2 p_r(I_{c_k,c_{k+1}}) \quad (6)$$

JTE
HCMUTE
ISSN: 2615-9740

JOURNAL OF TECHNICAL EDUCATION SCIENCE
Ho Chi Minh City University of Technology and Education
Website: https://jte.hcmute.edu.vn/
Email: jte@hcmute.edu.vn

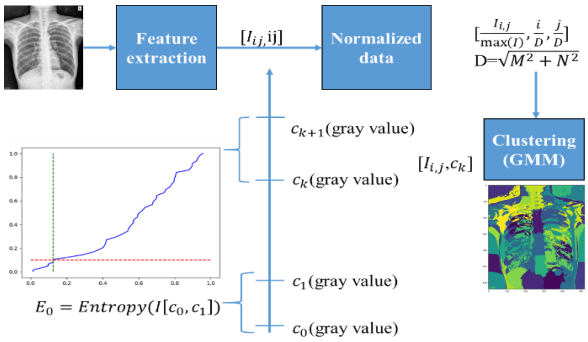

Figure 4. *Flowchart of estimating the important information area*

Here, $p_r(I_{c_k,c_{k+1}})$ denote the probability of the gray value r on the image $I_{c_k,c_{k+1}}$.

The cumulative $A_k = \sum_{l=0}^{k} E_{c_{l-1},c_l}$, therefore, measure the amount of information that could be lost if we ignore the gray values smaller than F_0^k. To measure the missing information in percent, the normalization of A_k could be estimated as $\bar{A}_k = A_k/\max(A_k)$.

Later, we apply the interpolation process [14] to render the curve as in Figure 4. The lower bound I_{im}^{min} is the maximum value such that the amount of lost information is less than a threshold δ <1 as shown in Equation (7).

$$I_{im}^{min} = arg \max_{F_0^k} A_k < \delta \tag{7}$$

3.3 Image quantization

In this section, we introduce the method to represent the important information range $[I_{im}^{min}, I_{im}^{max}]$ by multiple LDR images. Figure 5 shows the component images after extracting.

Given the range, we separate it into K sub-ranges $[I_l^{min}, I_l^{max}]\{l = 1\sim L\}$. Each sub-range is a low dynamic range that could be well presented in an 8-bit image. By using the quantization method, these LDR images are introduced by equations (8), (9), (10), (11). If l is small, the image given by Equ. (8) is bright because many pixels are greater than I_l^{max}. In this case, the lung region will be shown clearly. If l is great, the image is dark because many pixels are smaller than I_l^{min}. In this case, the bone in a very dense region is shown clearly.

$$I_l = 255 * min(1, max(0, \frac{I - I_l^{min}}{\Delta})) \tag{8}$$

$$\Delta = \frac{I_{im}^{max} - I_{im}^{min}}{L} \tag{9}$$

$$I_l^{max} = I_{im}^{max} + l\Delta \tag{10}$$

$$I_l^{min} = I_{im}^{min} + (l-1).\Delta \tag{11}$$

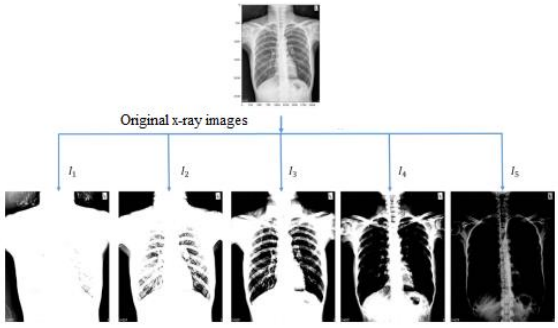

Figure 5. *Extracting component images from the original image*

JTE
HCMUTE
ISSN: 2615-9740

JOURNAL OF TECHNICAL EDUCATION SCIENCE
Ho Chi Minh City University of Technology and Education
Website: https://jte.hcmute.edu.vn/
Email: jte@hcmute.edu.vn

Here, I_l is the image that represents that sub-range $[I_l^{min}, I_l^{max}]$. In Equation (10)-(11), we may see that $I_l^{max} = I_{l+1}^{min}$, it means these sub-ranges will expand all over the important range. Furthermore, because the range of component images should not be less than 255 (8 bits), the maximum value of L is determined by equation (12).

$$L_{max} = \frac{I_{im}^{max} - I_{im}^{min}}{255} \quad (12)$$

3.4 Image fusion

Our result is an enhanced image that includes all information from the component LDR images. The mechanism in [8] is applied to fuse multi-component images into a unique one. Firstly, the quality of each pixel in component images is estimated through contrast score W^c [8] and saturation score W^s [8]. By using these two metrics, the quality-map is estimated as $W_{ij,k} = W_{ij,k}^c * W_{ij,k}^s$. Here, $i\ and\ j$ are the row and column of the k^{th} component image.

Using the quality map $W_{ij,k}$, we can represent the contribution of the k[th] image to the resulting image at location (i, j). The map $W_{ij,k}$ needs to be normalized to a weighted map as $\widehat{W}_{ij,k}$ that $\sum \widehat{W}_{ij,k} = 1$. This can be done via equation (13).

$$\widehat{W}_{ij,k} = [\sum_{k'}^{K=1} W_{ij,k'}]^{-1} W_{ij,k} \quad (13)$$

The final image R can be obtained by combining the weights of the input images as follows:

$$R_{ij} = \sum_{l=1}^{N} \widehat{W}_{ij,l}\, I_{ij,l} \quad (14)$$

As discussed in [8], due to unsmooth weighted maps, directly fusing sub-images will introduce some uncertainty results as in Figure 6. Hence, the input component images are decomposed into multiple lower resolution levels using the Laplacian pyramid [8] technique with M levels. Along with that, the weight map $\{\widehat{W}\}_{ij,l}^m$ is also decomposed into M lower resolution levels by the Gaussian pyramid technique [15]. At larger levels, the weight maps will be smoother due to the low resolution. The output image at each resolution is estimated by equation (15).

$$L\{R\}_{ij}^m = \sum_{l=1}^{N} G\,\{\widehat{W}\}_{ij,l}^m L\{I\}_{ij,l}^m \quad (15)$$

Finally, the enhanced result R for the m^{th} resolutions are estimated by Equ. (16). In this way, a high-resolution image will be generated by increasing the resolution of a low-resolution image and combining it with the detailed component of a high-resolution image$L\{R\}_{ij}^m$. In our work, the combination is represented by Equ.16. Here the α parameter controls the balance between the smooth term $R_{\uparrow}^{m+1}$ and the detailed term $L\{R\}_{ij}^m$.

$$R^m = \alpha R_{\uparrow}^{m+1} + (1-\alpha) L\{R\}_{ij}^m \quad (16)$$

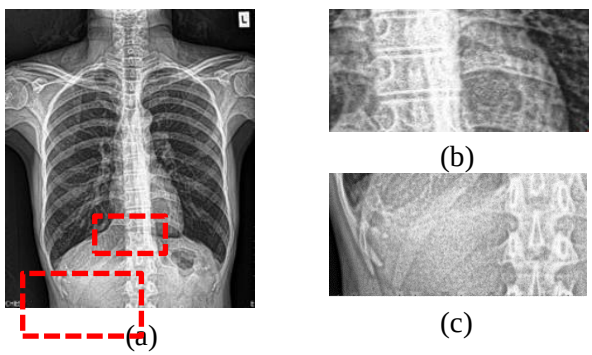

Figure 6. *The uncertainty result is given by directly fusing: (a) Enhanced image; (b) Zoom in lung (c) Zoom in the pelvis*

JTE HCMUTE
ISSN: 2615-9740
JOURNAL OF TECHNICAL EDUCATION SCIENCE
Ho Chi Minh City University of Technology and Education
Website: https://jte.hcmute.edu.vn/
Email: jte@hcmute.edu.vn

4. Experimental results

In this section, we demonstrate the effectiveness of the proposed method. The dataset is a subset of the data in [5]. The dataset [5] was collected at a Taiwan hospital and included 70 x-ray images from many human body parts. Because our work focuses on chest images, we randomly picked up 20 chest x-ray images to evaluate in our experiment. Qualitative and quantitative evaluations among the proposed method and well-known methods are presented in section 4.1. Moreover, the influence of control parameters is discussed in section 4.2 and section 4.3.

4.1 Compare with other methods

In the quantitative evaluation, seven metrics are used to compare these methods. The first metric is the contrast score. A higher contrast score means a better image. The second metric is the the Structural Similarity Index Measure (SSIM) [16] score. A higher SSIM means the pixel-wise relation is better. The third score is the Local-Brightness-Difference (LBD) [17] metric. A smaller LBD means the pixel-wise relation is well preserved. The four metrics are the Tenengrad (TEN) [18] that measures the sharpness of an image. A higher score means a better image quality. The fifth metric is the Discrete Entropy (DE) [19] that measures the amount of information in an image. A higher score DE means that the more information in the image. The sixth metric is the Measurement of Enhancement (EME) [20]. The higher score of this metric, the better the image enhancement performance. The final metric is the Absolute Mean Brightness Error (AMBE) [21] which is proposed to rate the performance in preserving the original brightness. Lower AMBE indicates that the brightness is better preserved.

Firstly, we compare the proposed method with well-known methods such as histogram equalization [1]. In addition, since the X-ray image is a high dynamic range image, the dynamic range compression methods [7] and [6] can also be used for image enhancement.

Moreover, we also compare our method with methods that are specifically designed for x-ray enhancement such as Koonsanit[3], Huang[5].

The result in Table 1 presents contrast, sharpness Tenengrad (TEN) [18], Local Brightness Difference (LBD) [17], Structural Similarity Index Measure (SSIM) [16], Discrete Entropy (DE) [19], Measurement of Enhancement (EME) [20], Absolute Mean Brightness Error (AMBE) [21] scores of these above methods. According to this result, traditional methods such as HE, Drago, and Duran do not achieve high contrast in x-ray image enhancement. In contrast, methods specially designed for a medical image, such as Koonsanit [3] and Huang [5] have higher contrast and sharpness. However, Koonsanit [3] only focuses on contrast enhancement but does not consider mass information. Therefore, its LBD is greatly overstated to 0.17. Huang's method [5] is designed to increase both contrast and preserve mass information. So it achieves very high contrast while keeping LBD lower than even traditional methods such as HE. Duran [6] and Drago [7] methods are HDR compression methods. It means the original image is presented in 16 bits. Hence, the local maximum is pretty high. In contrast, the enhanced or compressed image is an LDR image, and the local maximum is in the range [0-255]. Due to the phenomenon, we cannot use the LBD metric to evaluate the mass preserving property on HDR based method.

Table 1. *Comparison of image enhancement methods. (Red represents the best result, blue represents the second-best result.)*

	HE [1]	Dra [7]	Dur [6]	Koo [3]	Huang [5]	Our
Con	0.39	0.35	0.37	0.40	0.42	0.45
SSIM	0.82	0.66	0.66	0.83	0.59	0.61
LBD	0.12			0.17	0.11	0.10
TEN	5.24	4.47	4.98	5.51	5.87	5.60
DE	3.06	2.77	3.44	3.61	4.53	3.76
EME	31.21	53.63	55.36	36.21	55.62	64.10
AMBE	0.13			0.11	0.21	0.20

JTE
HCMUTE
ISSN: 2615-9740

JOURNAL OF TECHNICAL EDUCATION SCIENCE
Ho Chi Minh City University of Technology and Education
Website: https://jte.hcmute.edu.vn/
Email: jte@hcmute.edu.vn

Unlike HDR-based methods, other methods normalized the HDR image to a normalized LDR image. Later, an enhancement solution is applied. It means the original image and enhanced image are both in the LDR range. Because of this reason, we cannot compare our method with HDR-based methods in terms of LDR or AMBE metrics.

Unlike Huang[5], our method is designed to avoid missing information from original images. Since it relies on quality maps [8] to combine images, our method has much better contrast than traditional methods and is equivalent to Huang's method [5]. Besides, the recommended method has LBD slightly better than Huang [5]. Huang's LBD value is 0.11 while our method is 0.10.

In term of DE, and EME metrics, the results show that our method and Huang method are outperformance than others. In detail, Huang[5] method is better than the proposed method in term of DE metric; but our method is better in term of EME. In term of SSIM and AMBE, Huang[5] and our method is not better than conventional methods. The reason is that these methods focus on contrast enhancement but do not preserve the relationship among neighbor pixels or the brightness level. Therefore, the SSIM metric is not comparable with global transformation, where only one transformation is applied to an entire image. Behind the quantitative comparison, we provide another qualitative evaluation in Figure 7. Here, not only the full enhanced image is visualized, but a zoom-in result is also provided to demonstrate the performance of our method. The results show that although Huang [5] has higher contrast and sharpness, its appearance is unnatural.

In Figure 7(g), the area of the lungs, the gray levels inside and outside of the bones are relatively similar, but the gray level on the bone's edge is extremely high. In contrast, our method in Figure 7(h) ensures consistency inside and outside the bone region. Moreover, in Figure 7(i) and Figure 7(k), the pelvic area, Huang [5] method has better sharpness while our method has acceptable sharpness.

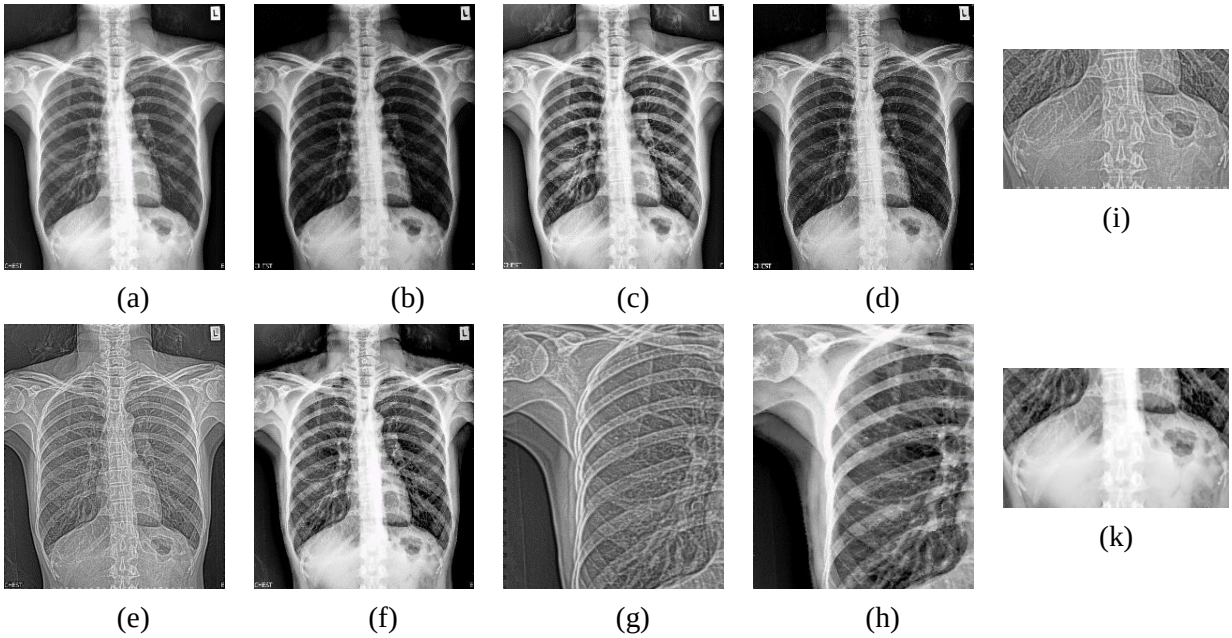

Figure 7. *Qualitative comparison between proposed method with other methods: (a) HE[1]; (b) Drago[7]; (c) Koonsanit[3]; (d) Durand[6]; (e) Huang[5]; (f) Proposed; (g) Zoom in lung area(Huang); (h) Zoom in lung area (Proposed Method); (i) Zoom in the pelvic area (Huang); (k)Zoom in the pelvic area (Proposed)*

4.2 Evaluate the effect of the lower threshold.

In this section, the influence of the lower bound is in section 3.2. We measure the LBD score given by various δ to explain the contribution of the lower bound. Experimental results are in figure 8. The results show that increasing the value will slightly reduce the LBD value to the lowest level. This demonstrates the possibility of choosing an appropriate lower bound to preserve mass information while achieving high contrast. Meanwhile, choosing δ too high will completely lose the meaning of preserving

JTE
HCMUTE
ISSN: 2615-9740

JOURNAL OF TECHNICAL EDUCATION SCIENCE
Ho Chi Minh City University of Technology and Education
Website: https://jte.hcmute.edu.vn/
Email: jte@hcmute.edu.vn

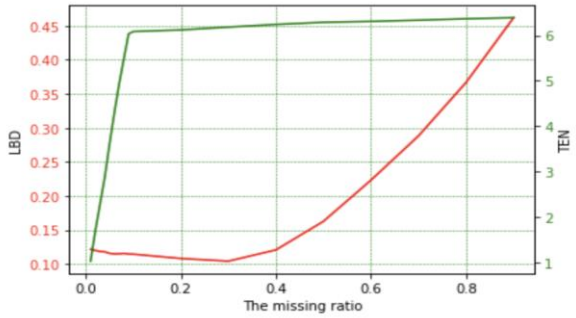

Figure 8. *Effect of δ on LDB and TEN*

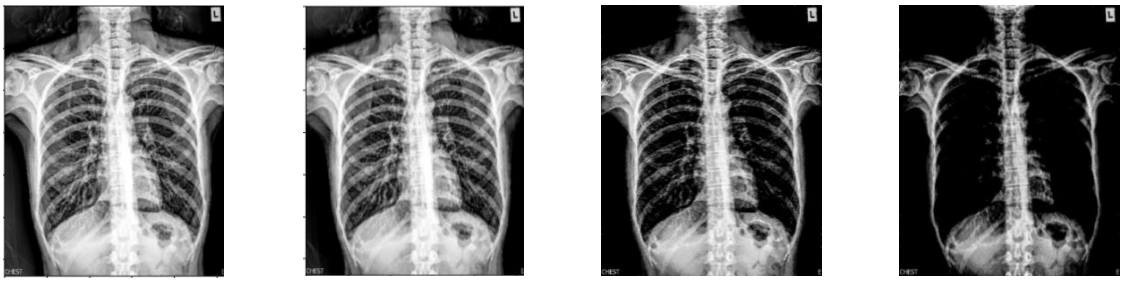

(a) (b) (c) (d)

Figure 9. *Results with different δ: (a) δ = 0.01; (b) δ = 0.1; (c) δ = 0.3; (d) δ = 0.7*

the image's information. Also, the TEN value could increase but not too much when the *δ is* greater than 0.1. Therefore, the optimal *δ* should be the value that minimum LBD. Moreover, we visualize some enhancement results with various δ in Figure 9.

The result shows that δ<0.1 may not affect the enhancement result. When δ is increased, the contrast will be better. A good result will be reached at δ = 0.3. If δ is large enough, a lot of information will be lost.For example, if δ = 0.7, all information in the lung area will be lost, and the LBD is extremely great.

4.3 Evaluate the effect of K coefficient

In this section, we evaluate the influence of the number of component images (K) on the performance. The contrast and SSIM indices are used for the quantitative evaluation. The results in Figure 10(a) show that the contrast score tends to increase as K increases, and SSIM tends to decrease. Because a well-enhanced image needs high contrast and high SSIM, then there is no optimal K that could be selected to enhance the image.

In this case, depend on our purpose, the K value should follow different selection strategies. To better understand how to select a suitable K value, a quantitative experiment is shown in Figure 10.

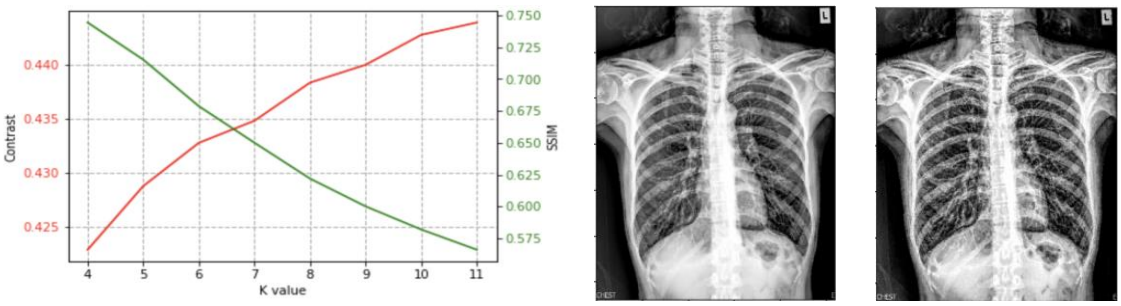

(a) (b) (c)

Figure 10. *Enhanced images with a different K value: (a) Effect of K on quality of the enhanced image (b) K=10; (c) K=4*

Here, the enhanced images corresponding with K=4 and K=10 are visualized. If K is greater (K=10), the contrast could be higher. More detail in the pelvic area could be observed when K=10. If K is smaller, the detail in the pelvic area is not clear, but the SSIM score is higher.

5. Conclusions

In this paper, we introduce an x-ray enhancement method based on important range and fusion mechanisms. Compared with traditional methods that linearly normalize DICOM images to LDR images, we analyzed the specific range that contains useful information of DICOM images. Consequently, our method has a better contrast than the original one. Besides, *the* experimental results demonstrate that the method is better than the existing methods in terms of preserving mass information (LBD). However, in term of SSIM metric, the proposed method cannot be comparable with the conventional method. Our future work will focus on how to ensure the information is preserved. Moreover, a deep learning framework will be used to enhance the chest x-ray image.

REFERENCES

[1] R. C. G. and R. E. Woods, *Digital image processing*, Upper Saddle River, N.J.: Prentice Hall, 2008.

[2] C. Lee, C. S. Kim, and C. Lee, "Contrast enhancement based on layered difference representation of 2D histograms," *IEEE Tran. Image Process.*, vol. 22, no. 12, 2013.

[3] K. Koonsanit, S.Thongvigitmanee, N. Pongnapang, and P. Thajchayapong, "Image enhancement on digital X-ray images using N-CLAHE," *10th Biomedical Engineering International Conference (BMEiCON)*, 2017.

[4] C. C. Huang, H. N. Manh, and C. Y. Tseng, "X-ray imaeg contrast enhancement based on tissue attenuation," *2014 IEEE International Conference on Acoustics, Speech and Signal Processing (ICASSP)*, 2014.

[5] C. C. Huang and M. H. Nguyen, "X-ray enhancement based on component attenuation, contrast adjustment, and image fusion," *IEEE Trans. Image Process.*, vol. 28, no. 1, 2019.

[6] F. Durand and J. Dorsey, "Fast bilateral filtering for the display of high-dynamic-range images," in ACM Transactions on Graphics, *ACM Journals*, vol.21,no.3, 2002.

[7] F. Drago, K. Myszkowski, T. Annen, and N. Chiba, "Adaptive Logarithmic Mapping for Displaying High Contrast Scenes," in *Computer Graphics Forum*, vol. 22, no. 3, 2003.

[8] T. Mertens, J. Kautz, and F. Van Reeth, "Exposure fusion: A simple and practical alternative to high dynamic range photography," *Comput. Graph. Forum*, vol. 28, no. 1, 2009.

[9] M. Gharbi, J. Chen, J. T. Barron, S. W. Hasinoff, and F. Durand, "Deep bilateral learning for real-time image enhancement," in *ACM Transactions on Graphics*, vol. 36, no. 4, 2017, doi: 10.1145/3072959.3073592.

[10] Y. Jiang *et al.*, "EnlightenGAN: Deep Light Enhancement without Paired Supervision," *IEEE Trans. Image Process.*, vol. 30, 2021, doi: 10.1109/TIP.2021.3051462.

[11] I. Y. Goodfellow, J. Pouget-Abadie, M. Mirza, B. Xu, D. Warde-Farley, S. Ozair, and et al, "Generative Adversarial Nets," *Proceedings of the International Conference on Neural*, Oct. 2014.

[12] T. Celik, "Spatial entropy-based global and local image contrast enhancement," *IEEE Trans. Image Process.*, vol. 23, no. 12, 2014.

[13] B. Yi, Z. Liu, G. Duan, and J. Tan, "Coarse-to-Fine Extraction of Free-Form Surface Features," *J. Comput. Inf. Sci. Eng.*, vol. 15, no. 1, 2015.

[14] G. Deslauriers and S. Dubuc, "Symmetric iterative interpolation processes," *Constr. Approx.*, vol. 5, no. 1, 1989.

[15] P. J. Burt and E. H. Adelson, "The Laplacian Pyramid as a Compact Image Code," *IEEE Trans. Commun.*, vol. 31, no. 4, 1983.

[16] Z. Wang, A. C. Bovik, H. R. Sheikh, and E. P. Simoncelli, "Image quality assessment: From error visibility to structural similarity," *IEEE Tran. Image Process.*, vol. 13, no. 4, 2004.

[17] W. Yang, L. Cai, and F. Wu, "Image segmentation based on gray level and local relative entropy two dimensional histogram," *PLoS One*, vol. 15, no. 3, 2020, doi: 10.1371/journal.pone.0229651.

[18] Z. Y. Chen, B. R. Abidi, D. L. Page, and M. A. Abidi, "Gray-level grouping (GLG): An automatic method for optimized image contrast enhancement - Part I: The basic method," *IEEE Trans. Image Process.*, vol. 15, no. 8, 2006, doi: 10.1109/TIP.2006.875204.

[19] C. E. Shannon, "A Mathematical Theory of Communication," *Bell Syst. Tech. J.*, vol. 27, no. 3, 1948.

[20] S. S. Agaian, B. Silver, and K. A. Panetta, "Transform coefficient histogram-based image enhancement algorithms using contrast entropy," *IEEE Tran. Image Process.*, vol. 16, no. 3, 2007.

[21] S. Der Chen and A. R. Ramli, "Minimum mean brightness error bi-histogram equalization in contrast enhancement," *IEEE Trans. Consum. Electron.*, vol. 49, no. 4, 2003.

Ngoc-Tham Vo received the B.S in electronic and telecommunication engineering from University of Technology and Education, Ho Chi Minh City, Vietnam, in 2017. He is currently a senior engineer as well as a postgraduate student at University of Technology and Education, Ho Chi Minh City. His research interests are in image processing and computer networking.

Email: tham.vongocpy@gmail.com

Mobile: 0866729909

Kim-Hoanh Ly received B.S in Mechatronics, University of Technology and Education, Ho Chi Minh city, Viet Nam, 2012. M.S in Mechatronics, Vietnamese German University, Binh Duong City, Viet Nam, 2016. Currently, he is a lecturer at University of Technology and Education, The University of Da Nang. His research interests are in robotics, image processing.

Email: lkhoanh@ute.udn.vn

Mobile: 0866279532

Manh-Hung Nguyen received the B.S., M.S. in electrical engineering from University of Technology and Education, Ho Chi Minh City, Vietnam, in 2009, 2011, respectively; and the Ph.D. degrees in electrical engineering from National Kaohsiung University of Applied Sciences, Taiwan, in 2016. He is currently an Assistant Professor with the Department of Electrical Engineering, University of Technology and Education, Vietnam; and Postdoc researcher in the Department of Electrical Engineering, National Chung Cheng University, Taiwan. His research interests are in machine learning and data analysis.

Email: hungnm@hcmute.edu.vn

Mobile: 0981977519